ELSEVIER

Atmospheric Environment 38 (2004) 2769–2777

ATMOSPHERIC ENVIRONMENT

www.elsevier.com/locate/atmosenv

Experimentally derived estimates of nitric acid dry deposition velocity and viscous sub-layer resistance at a conifer forest

S.C. Pryor[a,*], O. Klemm[b,1]

[a] *Atmospheric Science Program, Department of Geography, Indian University, 701 E. Kirkwood Avenue, Bloomington, IN 47405, USA*
[b] *University of Bayreuth, BITOeK, Germany*

Received 16 October 2003; received in revised form 19 February 2004; accepted 27 February 2004

Abstract

Daytime dry deposition of nitric acid to a conifer forest with a LAI of 5.3 was measured using the relaxed eddy accumulation technique. The observations indicate a mean friction velocity of $0.45\,m\,s^{-1}$and a mean dry deposition velocity (v_d) of $7.5\,cm\,s^{-1}$, with approximately equal aerodynamic (r_a) and non-aerodynamic resistances ($r_b + r_c$). Mean r_a is $10\,s\,m^{-1}$, while mean $r_b + r_c$ (derived from the difference between the observed v_d and a value derived based solely on r_a) is $13.2\,s\,m^{-1}$. Assuming the surface resistance (r_c) is zero, the viscous sub-layer resistance (r_b) from a number of models capture the mean observationally derived value to within $\pm 40\%$, but the models underestimate the variability inherent in the measurements. This discrepancy between the modeled and observed sample-to-sample variability of r_b does not appear to be accounted for by leaf wetness, stomatal opening or an additional dependence on friction velocity.

Keywords: HNO_3; Dry deposition; Flux; Relaxed eddy accumulation; Forest

1. Introduction

Nitrogen (N) availability is frequently observed to limit primary productivity and hence carbon (C) uptake in forests (Melillo, 1981). Anthropogenic activity has increased the emission of reactive N to the atmosphere (Galloway, 1998) and thus the supply of N to terrestrial ecosystems. Although the atmospherically derived N flux contribution to the total cycling of N in forest ecosystems may typically be small relative to internal N cycling, atmospheric deposition delivers N directly to the photosynthetically active foliage, especially the upper canopy and hence may have a disproportionate effect on N availability and partitioning. For example, Schulze (1989) has shown, for two Norway spruce stands, that 40–60% of atmospheric N deposition was retained in the canopy and could account for 8–20% of the annual N requirement for growth. It has thus been postulated that this increase in N supply to forests and particularly the direct atmosphere-canopy exchange of N may have stimulated increased C uptake by the recipient forests (Sievering et al., 2000).

Nitric acid (HNO_3) comprises a significant component of the total atmospheric burden of reactive N (Russell et al., 1993). During the daytime it is produced principally from oxidation of nitrogen dioxide (NO_2) by the hydroxyl radical (OH), while at night formation from dinitrogen pentoxide (N_2O_5), the nitrate radical and aqueous phase nitrate dominates (Finlayson-Pitts and Pitts, 2000). A significant fraction of HNO_3 removal from the atmosphere occurs via dry deposition as a result of its high surface affinity. Accordingly, most studies have resolved relatively high HNO_3 deposition velocities (v_d) to forests. For example:

(i) Meyers et al. (1989) reported a v_d of $2.2–6.0\,cm\,s^{-1}$ for a mixed species deciduous forest (described as 'oak-hickory' with patches of loblolly pine (*Pinus taeda*)) in southeastern USA.

*Corresponding author. Tel.: +1-812-855-5155; fax: +1-812-855-1661.

E-mail address: spryor@indiana.edu (S.C. Pryor).

[1] Now at University of Muenster, Institute for Landscape Ecology, Robert-Koch-str. 26, D-48149 Muenster, Germany.

1352-2310/$ - see front matter © 2004 Elsevier Ltd. All rights reserved.
doi:10.1016/j.atmosenv.2004.02.038

(ii) Sievering et al. (1994) report a mean v_d for total nitrate (HNO_3 plus particle nitrate) in a predominantly spruce forest (the BIATEX experimental forest) in southern Germany of 5.5 cm s^{-1}.

(iii) Sievering et al. (2001) report v_d values in the range of 0.8 to >20 cm s^{-1} to a mixed conifer forest (dominated by Engelmann spruce (*Picea engelmanni*), subalpine fir (*Abies lasiocarpa*) and lodgepole pine (*Pinus contorta*) trees) in the Rocky Mountain range of the USA.

(iv) Janson and Granat (1999) derived values of v_d of 3–11 cm s^{-1} for a Scots pine (*Pinus sylvestris*) forest in northern Sweden.

(v) Pryor et al. (2002) reported a mean v_d of 3 cm s^{-1} for HNO_3 to a mixed broadleaf forest (dominated by sugar maple (*Acer saccharum*), tulip poplar (*Liriodendron tulipifera*) sassafras (*Sassafras albidum*), white oak (*Quercus alba*), and black oak (*Q. velutina*)) in the Midwestern USA.

Studies (i)–(iii) used gradient techniques to derive their flux estimates, while (iv) used a foliar rinse technique and only the last study (v) used the relaxed eddy accumulation (REA) technique to directly determine the flux. Nevertheless, taken in concert with observations of elevated HNO_3 concentrations downwind of many urban environments (e.g. Bari et al., 2003; Janhall et al., 2003; Piringer et al., 1997; Russell et al., 1993; Stockwell et al., 2003) these studies imply HNO_3 may make a substantial contribution to total atmospheric N flux to forest ecosystems (Lindberg and Lovett, 1985). This flux may in turn be associated with impacts across a range of scales from cuticle damage on leaves (Bytnerowicz et al., 1998; Krywult et al., 1996) to modification of C:N ratios in foliage (Bytnerowicz et al., 1999) to changes in the N and C cycles within forests (Sievering et al., 2000).

Here we present research in which the REA technique was used to obtain direct estimates of the HNO_3 dry deposition flux to a coniferous forest in southern Germany during the daytime. These observational data and models from the literature are then used to examine this flux in more detail. Specifically, following work by Sievering et al. (2001), we use these data to examine the relative magnitude of aerodynamic and viscous sub-layer resistance in conifer forests and the relationship between observed and theorized values for the viscous sub-layer resistance. Then we explore hypotheses that have been advanced to explain discrepancies between modeled and observationally derived non-aerodynamic resistances to HNO_3 fluxes.

2. Methods

2.1. Experimental details

The measurements presented herein were conducted during May 2002 on a tower in the Waldstein forest in northeastern Bavaria, Germany (50°09′N, 11°52′E) at 765 m a.s.l. (Held et al., 2002a, b; Klemm and Mangold, 2001; Matzner, 2004). The forest is dominated by Norway spruce (*Picea abies*) and the leaf area index (LAI) during the measurement campaign was approximately 5.3. The experimental site is located within the "Lehstenbach" catchment 1 km to the SW of the "Bergkopf" summit (857 m a.s.l.) and slopes to the SSW with an angle of about 5°. The 30 m walk-up tower is located in a spruce stand of 50 years age and approximately 20 m height. At distances more than about 50 m to the W and E, respectively, the spruce tree height is 25–30 m. A 100 m × 100 m open field with forest nursery is located at a distance of 200 m to the W from the tower. A 6 m wide forest road crosses from WNW to ESE at a distance of 100 m from the tower. North of this road the 150-year-old spruce trees are about 27 m high and exhibit a relatively open trunk space.

Nitric acid fluxes were measured using REA which is a variant of eddy accumulation in which as the vertical velocity (w) exceeds a threshold ('dead-band') velocity, air is differentially sampled at a constant flow rate based on the vertical velocity (Businger and Oncley, 1990):

$$F = \overline{w'C'} = \beta\sigma_w(C_{up} - C_{down}), \quad (1)$$

where β is an experimental coefficient determined by the probability distribution of w, the dead-band width and sampling height. Here we use β as derived continuously based on the momentum and sensible heat fluxes (β_w and β_T), C_{up} and C_{down} are the average concentrations from samples collected when w is positive and negative, respectively, and σ_w the standard deviation of w.

The REA system deployed at the Waldstein forest has been previously described by Pryor et al. (2002) but in brief, the system has a dynamic dead-band of $\pm 0.5\sigma_w$, where σ_w is computed as a running mean over a period of 10 min. Use of a dynamic dead-band serves to maximize the difference in up and down channels (Bowling et al., 1999) which is particularly important in applications to forests that are very aerodynamically rough and hence are characterized by high turbulence resulting in much lower differences between the up and down collectors than over lower roughness surfaces. Use of a dynamic dead-band of $\pm 0.5\sigma_w$ as in the REA system applied here gives an approximate allocation of flow as follows; 30% to up-channel, 30% to down-channel, and 40% in the dead-band. The sample capture is on three sodium chloride coated denuders, one for updrafts, one for downdrafts and a third for constant sampling to derive an average concentration for the entire measurement period. To ensure laminar flow in the denuders they are flushed with HNO_3 free air when they are in a mode where ambient air is not sampled. After exposure the denuders are sealed and returned to the laboratory where they are extracted in de-ionized water and analysed by ion chromatography. Three

sample blanks were collected and used to correct the REA denuder concentrations for each sampling period. Concentrations on all REA denuders exceeded these sample blanks by a factor of 12 and most exceeded the blanks by more than a factor of 20.

The HNO_3 REA system was deployed at 32 m (above a canopy at 19–20 m) on the SW corner of the tower (the boom was oriented at 291°) and so experienced 'uninterrupted flow' from the south-west-north sector. In this paper we present daytime measurements which have a duration of between 1.5 and 5 h. The study design was to collect two daytime samples each day of sampling but sampling periods were modified/determined on the basis of prevailing meteorology to most closely achieve stationarity and open fetch conditions. Ozone (O_3) and carbon dioxide (CO_2) fluxes were also conducted during the sampling period using eddy covariance (see Klemm and Mangold, 2001 for details of the instrumental set up).

2.2. Calculation of dry deposition velocities

The rate of deposition in the absence of wet or occult processes is often specified as a dry deposition velocity (v_d) given by

$$v_d(z) = \frac{F}{C(z) - C(0)}, \quad (2)$$

where, $C(z)$ is the concentration at measurement height z, $C(0)$ the concentration at the surface (which may or may not be zero, depending on surface uptake) and F the flux or as a reciprocal of three serial resistances:

$$v_d(z) = \frac{1}{r_a(z) + r_b + r_c}, \quad (3)$$

where $r_a(z)$ is the aerodynamic resistance (f(surface roughness, height, stability, wind speed)), r_b the viscous sub-layer resistance (or quasi-laminar boundary layer resistance) (f(surface roughness, wind speed, chemical species)). This resistance describes the ease of transport across a largely 'turbulence free' sub-layer which forms above the receptor surface and r_c the surface or canopy resistance (f(surface type and conditions, chemical species)). For highly reactive or soluble gases the surface resistance is small. Many studies of deposition to forests assume that r_c for HNO_3 is zero (Hicks et al., 1987; Lovett, 1994; Meyers et al., 1989; Sievering et al., 2001), although Brook et al. (1999) used a value of 20 s m^{-1} for total surface resistance in their regional model to represent deposition to cuticle, soil and stomata.

Due to the preponderance of near-neutral stability during the Waldstein field experiment (Fig. 1), $r_a(z)$ is calculated using (Hicks et al., 1987):

$$r_a(z) = \frac{U(z)}{u_*^2}, \quad (4)$$

where $U(z)$ is the mean wind speed at height z and u_* the friction velocity.

'Observational' values for r_b are computed, under the assumption of $r_c = 0$, as

$$r_b = \frac{1}{v_d(z)} - r_a(z). \quad (5)$$

3. Results and discussion

3.1. Observed fluxes

As shown in Fig. 1 half-hour average friction velocity (u_*) during the field experiment varied up to 1 m s^{-1}, with a mean of approximately 0.45 m s^{-1}, although the mean wind speed at the instrument height was only 2.4 m s^{-1}. Conditions were generally characterized by near-neutral stability (based on the Monin–Obukhov length) and the flow direction varied but was from the west–northwest for extended periods giving an open fetch for the REA measurements. Although not a focus of this manuscript, both HNO_3 and O_3 exhibited periods of upward fluxes during the field experiment (Fig. 2). In the sample from 17 May the wind direction was such that flow to the REA may occasionally have been distorted by the tower. The other two cases with upward fluxes were also observed during the morning hours (approximately 8–11 a.m. (LT)) but the meteorological conditions do not imply flow distortion or non-stationarity. The magnitude of the difference between the up and down denuder channels ($C_{up} - C_{down}$) exceeds the individual analytical uncertainties associated with each HNO_3 denuder channel of ±5% for the concentrations observed. Both cases were associated with short periods of rapidly increasing in O_3 concentrations and on the 14 May simultaneous upward O_3 fluxes were observed. Gao et al. (1993) asserted on the basis of numerical modeling that, excluding reaction with NH_3 and partitioning to the particle phase, the HNO_3 v_d is relatively insensitive to near-canopy gas-phase chemistry. Reaction between NO_2 and OH to generate HNO_3 is discounted as a source of the observed upward fluxes observed here because it is relatively slow reaction and may be further limited by low OH concentrations near and within the canopy and also because this reaction would tend to lead to a decrease in O_3 concentrations due to the reduction in NO_2 concentrations and hence cannot account for the observed upward flux of O_3. Repartitioning of ammonium nitrate is also a possible source of HNO_3 (Kramm and Dlugi, 1994) but the increase of RH towards the canopy would tend of stabilize the particle phase. Release of HNO_3 due to hydrolysis of N_2O_5 in aqueous films on leaves (Finlayson-Pitts and Pitts, 2000) may act as a near-canopy source of HNO_3, although again this mechanism cannot

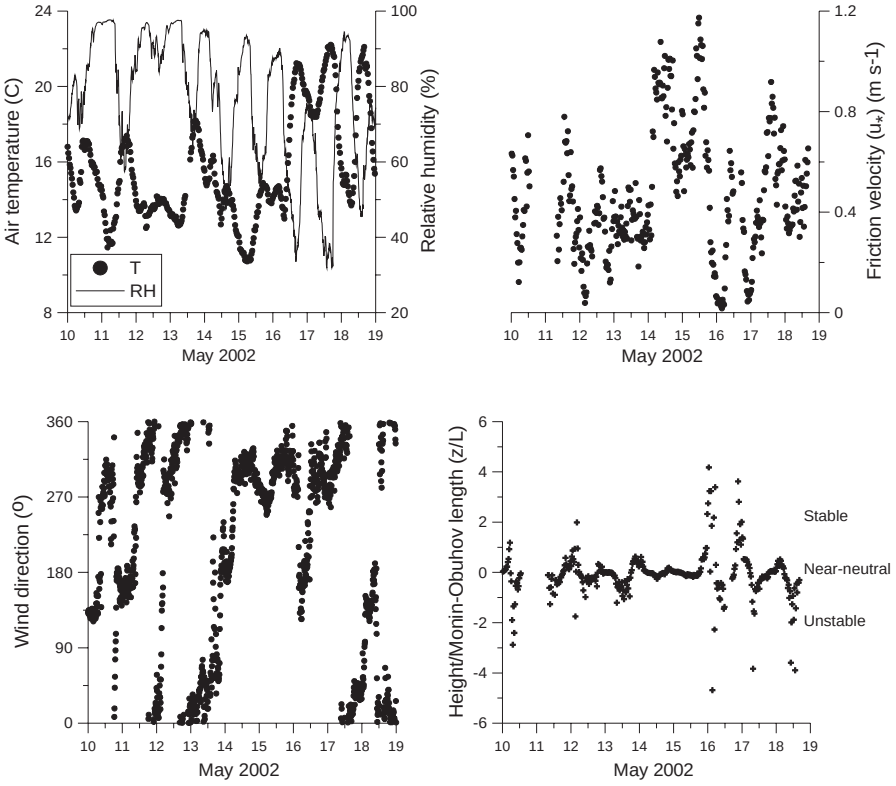

Fig. 1. Meteorological conditions during the experiment.

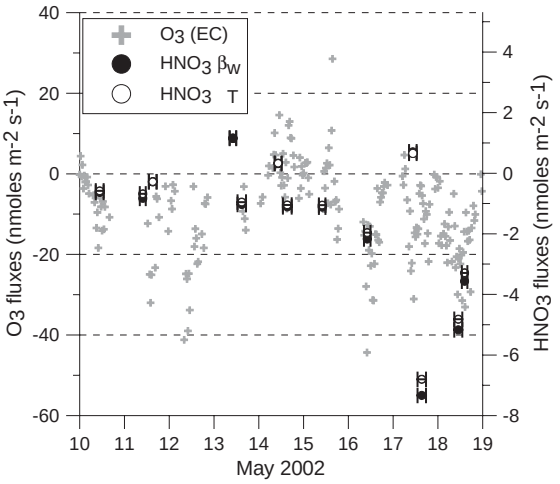

Fig. 2. Ozone fluxes from eddy covariance (EC) and HNO_3 fluxes using the REA technique using the momentum (β_w) and heat (β_T) analogies during the experiment. The horizontal bars on the HNO_3 fluxes indicate the sample duration.

explain the correspondence between the periods of O_3 and HNO_3 upward fluxes on 15 May. Alternatively upward fluxes of O_3 and HNO_3 may indicate incomplete scavenging by the canopy of aged polluted air vented to the near-surface during the breakdown of the nocturnal inversion. As described above, the forest exhibits considerable gapiness and horizontal advection of air parcels into the trunk space cannot be ruled out.

The mean HNO_3 flux for the daytime samples is $1.5\,\text{nmoles}\,\text{m}^{-2}\,\text{s}^{-1}$, with a mean associated v_d of $4.6\,\text{cm}\,\text{s}^{-1}$. If the cases of upward fluxes are omitted the mean resolved v_d is $7.5\,\text{cm}\,\text{s}^{-1}$. This value is in the midst of the values presented in Section 1 for conifer forests and, in accord with previous research, is higher than v_d derived by Pryor et al. (2002) for a deciduous forest using the same instrumentation.

3.2. Comparison of modeled and observationally derived of r_b

Previous work has suggested that the high observed HNO_3 v_d to conifer forests is due in part to the small aerodynamic needle width of conifer trees and hence the low r_b (Sievering et al., 2001). We compared observationally derived r_b estimates (calculated from Eq. (5)) to four commonly used formulations for r_b available in the literature (Table 1). For only one of the cases of downward fluxes does the observed v_d exceed the theorized maximum given by $v_d(z) = 1/r_a(z)$ (Fig. 3),

and this case exhibited the highest variability of wind speeds of all the sampling periods. For all other cases resolved r_b is positive.

The mean r_b from each of the models shows relatively close correspondence to the observationally derived value (Table 1). As in Sievering et al. (2001), the formulation proposed by Businger (1986) overestimates mean observationally derived r_b, while those of Hicks et al. (1987), Meyers et al. (1989) and Jensen and Hummelshoj (1995, 1997) underestimate mean r_b. From the difference of means, mean absolute difference and root mean square difference it appears the model of Jensen and Hummelshoj (1995, 1997) shows the lowest error relative to the observations, although the variations between model results are smaller than the observational uncertainty. As in the research of Sievering et al. (2001), the degree of sample-to-sample variability of resolved r_b is much higher in the observations than in the models (Fig. 4). One possible explanation for the lack of correspondence between the variability of the observations and models lies in the model formulations. The primary source of short-time scale variability in modeled r_b is via the dependence on $U(z)$ or u_*. In accord with theoretical research (Garratt and Hicks, 1973) observationally derived r_b is inversely related to u_* (increasing u_* may be associated with increased break down of quasi-laminar flow in this layer), but samples with similar u_* exhibit a high degree of variability in observationally derived r_b (Fig. 5). While it must be acknowledged that flux divergence may be an explanation for the difference between sample r_b from measurements and models, the good accord between the average values of r_b from the measurements and models implies this effect does not dominate the flux, and instead this observation may be interpreted as evidence that an additional source of short-term variability should be manifest in the models. For example, the characteristic canopy length scale as manifest in the r_b models of Jensen and Hummelshoj (1995, 1997) and Meyers et al. (1989), is commonly assumed in the case of conifer forest canopies to be the aerodynamic foliar width (Table 1). However, dry deposition occurs to all vegetation components, hence it is possible that some component of the high observed

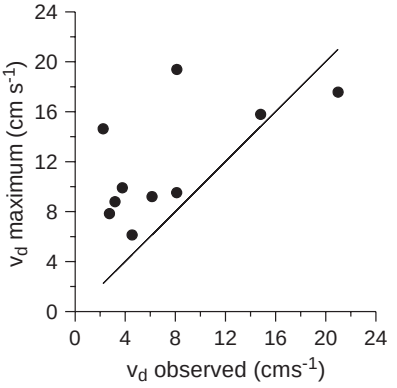

Fig. 3. Comparison of the observed HNO_3 v_d with a theoretical maximum calculated using $v_d(z) = 1/r_a(z), r_a(z) = U(z)/u_*^2$.

Table 1
Summary of the formulations of r_b used herein and statistics of the derived values relative to the observations ($n = 9$, the case where $v_d >$ theorized maximum has been excluded)

Observations		Mean ($s\,m^{-1}$)	Standard deviation ($s\,m^{-1}$)		
r_a		10.0	3.5		
r_b		13.2	12.4		
Source	Formulation	Mean modeled r_b ($s\,m^{-1}$)	Standard deviation ($s\,m^{-1}$)	RMSD[a] ($s\,m^{-1}$)	MAD ($s\,m^{-1}$)
Businger (1986)	$r_b = 10.2u_*^{-2/3}$	16.6	3.8	12.7	10.2
Hicks et al. (1987)	$r_b = \frac{2}{\kappa u_*}\left(\frac{Sc}{Pr}\right)^{2/3}$	10.6	3.6	12.5	9.9
Jensen and Hummelshoj (1995, 1997)	$r_b = \frac{v}{D}\left[\frac{c}{(\mathrm{LAI})^2}\left(\frac{lu_*}{v}\right)\right]^{1/3}\frac{1}{u_*}$	12.4	2.8	12.0	9.7
Meyers et al. (1989)	$r_b = \frac{1}{D0.66\left(\frac{Ul}{v}\right)^{1/2}\left(\frac{v}{D}\right)^{1/3}}$	9.5	1.6	12.2	9.5

[a] RMSD is the root mean square difference: $\sqrt{\overline{(\mathrm{Observed} - \mathrm{modeled})^2}}$, MAD the mean absolute difference: $\overline{|\mathrm{Observed} - \mathrm{modeled}|}$, where $u*$ is the friction velocity, κ the von Karman constant (0.4), Sc the Schmidt number (v/D), Pr the Prandlt number (v/k) ≈ 0.72 (Hicks et al., 1987), v the kinematic viscosity of air ($1.4607 \times 10^{-5}\,m^2\,s^{-1}$), D the diffusivity (a value of $12\,mm^2\,s^{-1}$ was used here), k the thermal diffusivity, LAI the leaf area index (a value of 5.3 was used here), l the characteristic leaf width (a value of 1 mm was used here), c is a constant (a value of 100 was used here) and U the wind speed.

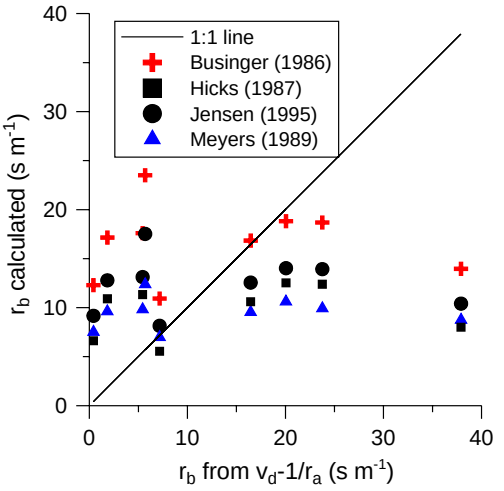

Fig. 4. r_b for each sample as derived from the observed HNO_3 fluxes and as calculated using the four models described in Table 1.

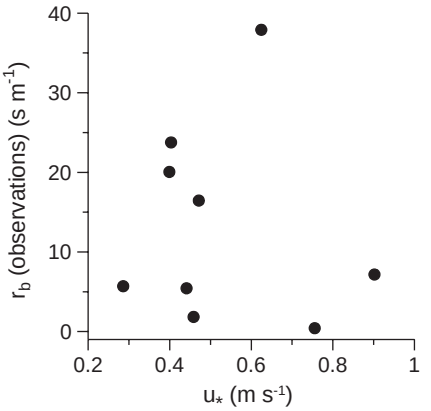

Fig. 5. r_b for each sample as derived from the observed HNO_3 fluxes versus the sample mean friction velocity (u_*).

r_b variability may reflect the influence of flow variability as it interacts with apparent deposition surface area.

3.3. Consideration of r_c

Analysis in Section 3.2, like many previous studies, assumed the surface resistance to HNO_3 uptake by forests is zero (Meyers et al., 1989; Sievering et al., 2001). However, a possible explanation for the lack of correspondence between observed and modeled values for the r_b and particularly the variability of the observationally derived r_b may lie in variations in the surface resistance (or conductivity), and hence r_c. Indeed, Tarnay et al. (2002) used data collected using an open gas exchange system to derive cuticular resistances for California red fir (*Abies magnifica*), California white fir (*Abies concolor*) and Jeffrey pine (*Pinus jeffreyi*) seedlings of 20–184 s m^{-1} for HNO_3 concentrations of 1–13 ppb and relative humidity (RH) below 20%. Although these results may not be directly applicable to atmospheric conditions where such low RH is seldom observed (RH during the Waldstein experiment ranged between 30% and 95% (Fig. 1)) and increasing RH may lead to decrease in this resistance due to formation of thin water films (Burkhardt and Eiden, 1994), it is worthy of note that the entire range of cuticular resistance determined by Tarnay et al. (2002) exceeds both the mean r_a and r_b derived for the Waldstein data.

Differing studies have provided evidence for uptake of HNO_3 via (a) adsorption onto the leaf and other surfaces (Janson and Granat, 1999), trans-cuticular transport (i.e. diffusion through the cuticle primarily across the lipophilic phase of the cuticle (Marshall and Cadle, 1989) and into the foliage) and uptake via stomata (Hanson and Garten, 1992). Both of the latter could account for the observation that HNO_3 dry deposition to forests is associated with an increase in nitrate reductase (NR) activity in leaves on time scales of a few minutes (Krywult and Bytnerowicz, 1997). The relative importance of these pathways shows variation with:

(i) Plant genus and leaf/canopy morphology and age. Total canopy uptake varies by species (Dasch, 1989; Hanson and Garten, 1992; Krywult and Bytnerowicz, 1997) and absorption rates differ with exposure according to foliage age (Vose and Swank, 1990). Typically, deciduous species exhibit greater 'binding' of deposited HNO_3 into foliage (Hanson and Garten, 1992).

(ii) Duration of exposure (decreasing adsorption as adsorption sites become saturated) (Marshall and Cadle, 1989).

(iii) Location in the canopy (Janson and Granat, 1999). Bytnerowicz et al. (1999) used profile measurements of HNO_3 concentrations on a vertical transect to infer that 'HNO_3 conductance or deposition velocity at a single branch level were significantly higher at the canopy top as compared with lower branches.' This they attributed to higher wind speeds in the upper canopy.

(iv) Environmental conditions such as (a) leaf wetness and (b) light level. Leaf-level uptake of HNO_3 and other acidifying gases has also been demonstrated to be dependent on leaf wetness (Dasch, 1989) due, at least in part, to the aqueous phase chemistry within the water layer (Chameides, 1987; Zhang et al., 2003). The apparent dependence on illumination conditions illustrated in laboratory experiments may imply some degree of stomatal control (Hanson and Garten, 1992; Krywult et al., 1996). In their study of HNO_3 uptake by dormant shoots of 2-year-old eastern white pine (*Pinus*

strobus) seedlings under dark conditions Marshall and Cadle (1989) documented only 5–9% of HNO_3 migrated into the leaf proper (via diffusing across the cuticle), while Cadle et al. (1991) presented a laboratory study which indicated a higher fraction of non-adsorption uptake under illuminated conditions. This is not definitive evidence of stomatal uptake and Dasch (1989) suggests that although their data showed a positive correlation between inferred stomatal and total deposition velocities these results may reflect 'a relationship between function of the leaf and the cuticular deposition' rather than a direct stomatal control.

The experimentally derived values of r_b were examined in light of this previous research. On the basis of this analysis the following observations can be made. 'Observed' r_b did not exhibit a trend towards increased resistance over the course of the field experiment and this coupled with the relatively low mean HNO_3 concentration during the REA flux measurement periods of approximately 32 nmoles m^{-3} ($\sim 2\,\mu g\,m^{-3}$) implies that saturation of adsorption sites was not a cause of the sample-to-sample variability in resolved r_b. It has been shown that thin water films form on spruce needles at RH as low as 50% (Burkhardt and Eiden, 1994) and that these films can substantially affect gas deposition (Chameides, 1987) even from relatively low solubility gases (Fuentes et al., 1992; Wesley, 1989). Accordingly, leaf wetness is routinely sampled at the Waldstein experimental site (Klemm et al., 2002). However, these data indicate little sample-to-sample variability of leaf wetness and only one of the nine samples corresponded to completely wet leaves. In contrast to apriori expectations this sample shows the highest observed r_b, which may reflect a reduction in surface uptake due to a reduction in diffusion into the leaf interior or acidification of liquid layers by deposition of other gases (Chameides, 1987). Excluding this one sample leaf-wetness it is thus asserted that leaf-wetness was not the cause of the observed variability in r_b. The possible role of co-deposition (Erisman and Wyers, 1993) or prior deposition of basic compounds in enhancing deposition could not be examined due to the lack of data to quantify these effects. Coincident measurements of O_3 and CO_2 fluxes which are both largely mediated by stomatal opening (Arain et al., 2002; Lamaud et al., 2002) (Fig. 6) do not appear to vary according to the magnitude of the observed r_b for HNO_3. This implies that stomatal opening is also not a major determinant of sample-to-sample variability in the daytime HNO_3 fluxes observed at the Waldstein.

To further investigate possible causes of the differences between predicted and observed r_b and the possible effect of co-variation of potential controlling parameters, the meteorological and chemical data from each sample period were subjected to principal components analysis (Richman, 1986). This analysis did not yield any further explanation of the short-term (sample-to-sample) variability of r_b in terms of these environmental parameters possibly due to the small sample size.

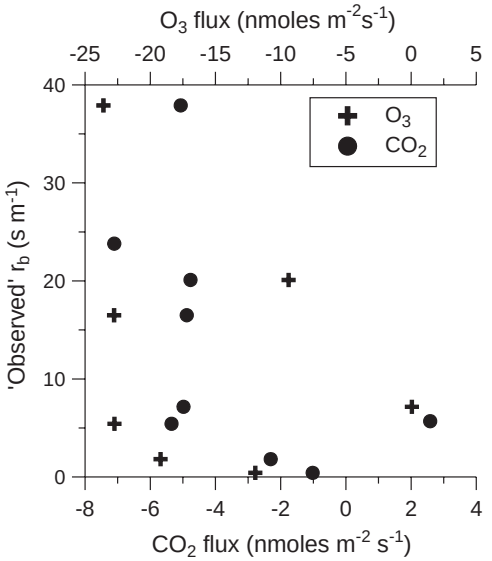

Fig. 6. Observed HNO_3 r_b for each sample versus the mean flux of ozone (O_3) and carbon dioxide (CO_2) for coincident measurements.

4. Summary and concluding remarks

We present HNO_3 fluxes to a conifer forest with a LAI of 5.3 obtained by application of the REA technique. The results indicate a mean v_d of 7.5 cm s^{-1}, and approximately comparable aerodynamic and viscous sub-layer resistances (mean $r_a = 10\,s\,m^{-1}$, mean $r_b = 13.2\,s\,m^{-1}$). Experimentally derived estimates of r_b are compared with four model formulations from the literature. As in the research of Sievering et al. (2001), the results indicate that while all the models capture the mean r_b to within $\pm 40\%$ of the observed value, the variability manifest in the observations is not captured by the models. Possible sources of this variability include; (i) insufficient sensitivity of the r_b models to factors that cause short-term variability and (ii) non-zero and varying surface resistance (r_c). While no definitive explanation for the difference in variability is reached, the observational data do not support postulates involving greater sensitivity to friction velocity, saturation of adsorption sites, significant stomatal control on HNO_3 v_d, or that varying leaf wetness as the source of the observed variability, and application of multivariate statistical techniques did not yield any further explanation of the short term (sample-to-sample)

variability of r_b in terms of these or other environmental parameters. The lack of a definitive explanation for the high variability of r_b may reflect the small sample size. Nevertheless these data provide independent confirmation of inferences drawn from data presented in Sievering et al. (2001), and given the reported importance of HNO_3 in the budget of atmospheric N supply to forests they emphasize the need for further research to quantify and parameterize the HNO_3 viscous sub-layer resistance and dry deposition velocity for forests.

Acknowledgements

This research was funded in part by Grants to SP from NSF (ATM 9977281 and ATM 0334321), the National Institute for Global Environmental Change (NIGEC) through the US DoE (cooperative agreement DE-FC03-90ER61010), and fellowships to SP from the University of Bayreuth and the Nordic Centre of Excellence on Biosphere–Aerosol–Cloud–Climate Interactions (BACCI). This work was also supported in part by the German federal Bundesministerium für Bildung und Forschung (BMBF) through Grant No. PT BEO 51-0339476 C. The authors gratefully acknowledge logistical support from Lise Lotte Sørensen, analytical support from Rebecca Barthelmie, review comments from Rebecca Barthelmie, Sven Erik Gryning and two anonymous reviewers, and technical support from Bjarne Jensen.

References

Arain, M.A., et al., 2002. Effects of seasonal and interannual climate variability on net ecosystem productivity of boreal deciduous and conifer forests. Canadian Journal of Forest Research 32, 878–891.

Bari, A., Ferraro, V., Wilson, L., Luttinger, D., Husain, L., 2003. Measurements of gaseous HONO, HNO_3, SO_2, HCl, NH_3, particulate sulfate and PM2.5 in New York, NY. Atmospheric Environment 37, 2825–2835.

Bowling, D.R., Delany, A.C., Turnispeed, A., Baldocchi, D., Monson, R., 1999. Modification of the relaxed eddy accumulation technique to maximize measured scalar mixing ratio differences in updraft and downdrafts. Journal of Geophysical Research 104, 9121–9133.

Brook, J.R., Zhang, L., Di-Giovanni, F., Padro, J., 1999. Description and evaluation of a model of deposition velocities for routine estimates of air pollutant dry deposition over North America. Part I: model development. Atmospheric Environment 33, 5037–5051.

Burkhardt, J., Eiden, R., 1994. Thin water films on coniferous needles (with an Appendix " a new device for the study of water vapour condensation and gaseous deposition to plant surfaces and particle samples" by J. Burkhardt, and J. Gerchau). Atmospheric Environment 28, 2001–2017.

Businger, J.A., 1986. Evaluation of the accuracy with which dry deposition can be measured with current micrometeorological techniques. Journal of Climate and Applied Meteorology 25, 1100–1124.

Businger, J.A., Oncley, S.P., 1990. Flux measurement with conditional sampling. Journal of Atmospheric and Oceanic Technology 7, 349–352.

Bytnerowicz, A., Percy, K., Riechers, G., Padgett, P., Krywult, M., 1998. Nitric acid vapor effects on forest trees-deposition and cuticular changes. Chemosphere 36, 697–702.

Bytnerowicz, A., et al., 1999. Direct effects of nitric acid on forest trees. In: Miller, P., McBride, J. (Eds.), Oxidant Air Pollution Impacts on the Montane Forests of Southern California. Springer, New York, pp. 270–287.

Cadle, S.H., Marshall, J.D., Mulawa, P.A., 1991. A laboratory investigation of the routes of HNO_3 dry deposition to coniferous seedlings. Environmental Pollution 72, 287–305.

Chameides, W.L., 1987. Acid dew and the role of chemistry in the dry deposition of reactive gases to wetted surfaces. Journal of Geophysical Research 92, 11895–11908.

Dasch, J.M., 1989. Dry deposition of sulfur dioxide or nitric acid to Oak, Elm and Pine leaves. Environmental Pollution 59, 1–16.

Erisman, J.W., Wyers, G.P., 1993. Continuous measurements of surface exchange to SO_2 and NH_3: implications for their possible interactions in the deposition process. Atmospheric Environment 27A, 1937–1949.

Finlayson-Pitts, B.J., Pitts, J.N., 2000. Chemistry of the Upper and Lower Troposphere. Academic Press, San Diego, 969 pp.

Fuentes, J.D., Gillespie, T.J., den Hartog, G., Neumann, H.H., 1992. Ozone deposition onto a deciduous forest during dry and wet conditions. Agricultural and Forest Meteorology 62, 1–18.

Galloway, J.N., 1998. The global nitrogen cycle: changes and consequences. Environmental Pollution 102, S1, 15–24.

Gao, W., Wesely, M.L., Doskey, P.V., 1993. Numerical modeling of the turbulent diffusion and chemistry of NO_x, O_3, isoprene, and other reactive trace gases in and above a forest canopy. Journal of Geophysical Research: Atmosphere 98, 18339–18353.

Garratt, J., Hicks, B., 1973. Momentum, heat and water vapour transfer to and from natural and artificial surfaces. Quarterly Journal of the Royal Meteorological Society 99, 680–687.

Hanson, P., Garten, C., 1992. Deposition of $H_{15}NO_3$ vapour to white oak, red maple and loblolly pine foliage: experimental observations and a generalized model. New Phytologist 122, 329–337.

Held, A., Hinz, K., Trimborn, A., Spengler, B., Klemm, O., 2002a. Chemical classes of atmospheric aerosol particles at a rural site in central Europe during winter. Journal of Aerosol Science 33, 581–594.

Held, A., Wrzesinsky, T., Mangold, A., Gerchau, J., Klemm, O., 2002b. Atmospheric phase distribution of oxidized and reduced nitrogen at a forest ecosystem research site. Chemosphere 48, 697–706.

Hicks, B.B., Baldocchi, D.D., Meyers, T.P., Hosker, R.P., Matt, D.R., 1987. A preliminary multiple resistance routine for deriving dry deposition velocities. Water, Air and Soil Pollution 36, 311–330.

Janhall, S., Molnar, P., Hallquist, M., 2003. Vertical distribution of air pollutants at the Gustavii Cathedral in Goteborg, Sweden. Atmospheric Environment 37, 209–217.

Janson, R., Granat, L., 1999. A foliar rinse study of the dry deposition of nitric acid to a coniferous forest. Agricultural and Forest Meteorology 98–99, 683–696.

Jensen, N.O., Hummelshoj, P., 1995. Derivation of canopy resistance for water vapour fluxes over a spruce forest using a new technique for the viscous sublayer resistance. Agricultural and Forest Meteorology 73, 339–352.

Jensen, N.O., Hummelshoj, P., 1997. Erratum to 'Derivation of canopy resistance for water vapour fluxes over a spruce forest using a new technique for the viscous sublayer resistance'. Agricultural and Forest Meteorology 85, 289.

Klemm, O., Mangold, A., 2001. Ozone deposition at a forest site in NE Bavaria. Water, Air and Soil Pollution 1, 223–232.

Klemm, O., Milford, C., Sutton, M., Spindler, G., van Putten, E., 2002. A climatology of leaf surface wetness. Theoretical and Applied Climatology 71, 107–117.

Kramm, G., Dlugi, R., 1994. Modelling the vertical fluxes of nitric acid, ammonia and ammonium nitrate. Journal of Atmospheric Chemistry 18, 319–357.

Krywult, M., Bytnerowicz, A., 1997. Induction of nitrate reductase activity by nitric acid vapor in California black oak (*Quercus kelloggii*) canyon live oak (*Quercus chrysolepis*) and ponderosa pine (*Pinus ponderosa*) seedlings. Canadian Journal of Forest Research 27, 2101–2104.

Krywult, M., Horn, J., Bytnerowicz, A., Percy, K., 1996. Deposition of gaseous nitric acid and its effects on foliage of Ponderosa Pine (*Pinus ponderosa* Dougl. ex Laws.) seedlings. In: Cox, R.A., Percy, K., Jensen, K., Simpson, C. (Eds.), Air Pollution and Multiple Stresses: 16th International meeting for specialists in Air Pollution Effects on Forest Ecosystems, Fredericton, New Brunswick, Canada, pp. 45-51.

Lamaud, E., Carrar, A., Brunet, Y., Lopez, A., Druilhet, A., 2002. Ozone fluxes above and within a pine forest canopy in dry and wet conditions. Atmospheric Environment 36, 77–88.

Lindberg, S., Lovett, G.M., 1985. Field measurements of dry deposition to foliage and inert surfaces in a forest canopy. Environmental Science and Technology 19, 238–244.

Lovett, G.M., 1994. Atmospheric deposition of nutrients and pollutants in North America: an ecological perspective. Ecological Applications 4, 629–650.

Marshall, J.D., Cadle, S.H., 1989. Evidence for trans-cuticular uptake of HNO_3 vapor by foliage of eastern White Pine (*Pinus strobus* L.). Environmental Pollution 60, 15–28.

Matzner, E. (Ed.), 2004. Biogeochemistry of forested catchments in a changing environment: a case study in NE-Bavaria, Germany. Ecological Studies. Springer Verlag, Berlin, in press.

Melillo, J.M., 1981. Nitrogen cycling in deciduous forests. Ecological Bulletin 33, 427–442.

Meyers, T.P., Huebert, B.J., Hicks, B.B., 1989. HNO_3 deposition to a deciduous forest. Boundary-Layer Meteorology 49, 395–410.

Piringer, M., Ober, E., Puxbaum, H., Kromp-Kolb, H., 1997. Occurrence of nitric acid and related compounds in the northern Vienna basin during summertime anticyclonic conditions. Atmospheric Environment 31, 1049–1057.

Pryor, S.C., Barthelmie, R.J., Jensen, B., Jensen, N.O., Sørensen, L.L., 2002. HNO_3 fluxes to a deciduous forest derived using gradient and REA methods. Atmospheric Environment 36, 5993–5999.

Richman, M.B., 1986. Rotation of principal components. Journal of Climatology 6, 293–335.

Russell, A.M., Winner, D., Harley, R., McCue, K., Cass, G., 1993. Mathematical modeling and control of the dry deposition flux of nitrogen containing air pollutants. Environmental Science and Technology 27, 2772–2782.

Schulze, E., 1989. Air pollution and forest decline in a spruce forest. Science 244, 776–783.

Sievering, H., et al., 1994. Nitric acid, particulate nitrate and ammonium profiles at the Bayerischer Wald: evidence for large deposition rates of total nitrate. Atmospheric Environment 28, 311–315.

Sievering, H., Fernandez, I., Lee, J., Hom, J., Rustad, L., 2000. Forest canopy uptake of atmospheric nitrogen deposition at eastern US conifer sites: carbon storage implications? Global Biogeochemical Cycles 14, 1153–1160.

Sievering, H., Kelly, T., McConville, G., Seibold, C., Turnipseed, A., 2001. Nitric acid dry deposition to conifer forests: Niwot Ridge spruce-fir-pine study. Atmospheric Environment 35, 3851–3859.

Stockwell, W.R., et al., 2003. The Treasure Valley secondary aerosol study II: modeling of the formation of inorganic secondary aerosols and precursors for southwestern Idaho. Atmospheric Environment 37, 525–534.

Tarnay, L., Gertler, A., Taylor, G.E., 2002. The use of inferential models for estimating nitric acid vapor deposition to semi-arid coniferous forests. Atmospheric Environment 36, 3277–3287.

Vose, J.M., Swank, W.T., 1990. Preliminary estimates of foliar absorption of 15N-labeled nitric acid vapor (HNO_3) by mature eastern white pine (*Pinus strobus*). Canadian Journal of Forest Research 20, 857–860.

Wesley, M.L., 1989. Parameterization of surface resistances to gaseous dry deposition in regional scale numerical models. Atmospheric Environment 23, 1293–1304.

Zhang, L., Brook, J.R., Vet, R., 2003. Evaluation of a nonstomatal resistance parameterization for SO_2 dry deposition. Atmospheric Environment 37, 2941–2947.